Ultrasonics Sonochemistry 77 (2021) 105700

Contents lists available at ScienceDirect

Ultrasonics Sonochemistry

journal homepage: www.elsevier.com/locate/ultson

Effect of ultrasound on the preparation of soy protein isolate-maltodextrin embedded hemp seed oil microcapsules and the establishment of oxidation kinetics models

Tong Wang [a], Kuiren Chen [a], Xingzhen Zhang [a], Yingjie Yu [a], Dianyu Yu [a,*], Lianzhou Jiang [a,*], Liqi Wang [b]

[a] School of Food Science, Northeast Agricultural University, Harbin 150030, China
[b] School of Computer and Information Engineering, Harbin University of Commerce, Harbin 150028, China

ARTICLE INFO

Keywords:
Microcapsules
Ultrasonic treatment
Hemp seed oil
Soy protein isolate
Maltodextrin
Oxidation kinetics

ABSTRACT

In this study, microcapsules were prepared by spray drying and embedding hemp seed oil (HSO) with soy protein isolate (SPI) and maltodextrin (MD) as wall materials. The effect of ultrasonic power on the microstructure and characteristics of the composite emulsion and microcapsules was studied. Studies have shown that ultrasonic power has a significant impact on the stability of composite emulsions. The particle size of the composite emulsion after 450 W ultrasonic treatment was significantly lower than the particle size of the emulsion without the ultrasonic treatment. Through fluorescence microscopy observation, HSO was found to be successfully embedded in the wall materials to form an oil/water (O/W) composite emulsion. The spray-dried microcapsules showed a smooth spherical structure through scanning electron microscopy (SEM), and the particle size was 10.7 μm at 450 W. Fourier transform infrared (FTIR) spectroscopy analysis found that ultrasonic treatment would increase the degree of covalent bonding of the SPI-MD complex to a certain extent, thereby improving the stability and embedding effect of the microcapsules. Finally, oxidation kinetics models of HSO and HSO microcapsules were constructed and verified. The zero-order model of HSO microcapsules was found to have a higher degree of fit; after verification, the model can better reflect the quality changes of HSO microcapsules during storage.

1. Introduction

Hemp is a one-year-old herb, from which hemp seeds can be used in food fields after processing. Hemp seed is rich in oil, usually between 30% and 35% [1]. Hemp seed oil (HSO) is composed mainly of monounsaturated fatty acids and polyunsaturated fatty acids, and the content is as high as 80% [2]. HSO is also rich in trace elements, γ-linolenic acid, and bioactive ingredients such as tocopherols and phytosterols [3], which have good anti-inflammatory [4], antioxidant [5], memory improvement [6] and other effects. Therefore, HSO is a high-quality functional oil [7]. Tetrahydrocannabinol (THC) is a unique psychoactive ingredient in hemp seeds [8], and its content in HSO is <0.3% [9], which complies with European Union and United States standards [10] and has a certain medicinal value [11,12]. However, polyunsaturated fatty acids in HSO are prone to oxidative degradation during food processing, transportation and storage [13], leading to the loss of their biological function, which brings huge challenges to the application of HSO in functional foods.

As a new type of embedding technology, microencapsulation can make the core of the capsule embedded in the wall material isolated from the external environment, and protected from the influence of adverse factors [14], so microencapsulation is widely used in the food field [15]. Applying the technology to oils can slow down the oxidative degradation of oils during processing and storage [16]. The common method of microencapsulation is spray drying, which can convert liquid into powder with a rapid drying speed, less nutrient loss, and lower production cost, making the microcapsules easier to process, store and transport [17,18]. Studies have found that soy protein isolate (SPI) is a vegetable protein with good emulsifying properties and stability [19,20] and has the advantages of good processing performance, high nutritional value, and low cost. Therefore, SPI is an ideal wall material for microencapsulation. Maltodextrin (MD) is a partial hydrolysis product

* Corresponding authors.
E-mail addresses: dyyu2000@126.com (D. Yu), jlzname@163.com (L. Jiang).

https://doi.org/10.1016/j.ultsonch.2021.105700
Received 20 May 2021; Received in revised form 23 July 2021; Accepted 27 July 2021
Available online 30 July 2021

of starch that is usually used as a secondary wall material for spray drying and microencapsulation. MD has the advantages of low cost, neutral aroma and taste, low viscosity at high solid phase concentration, and good antioxidant properties [21], so it can combine with protein to improve the encapsulation effect of microcapsules.

Ultrasound is a sound wave with a frequency higher than 20000 Hz [22] that has good transmission and reflection capabilities. Compared with other technologies, phacoemulsification technology has great advantages, due mainly to its energy savings, low production cost, and ease of operation and control [23]. Ultrasound is widely used in the physical processing of food, especially in recent years, and it is often used for the extraction and modification of dietary fiber, polysaccharides, protein and various food functional components [24,25]. Huang et al. [26] found that ultrasonication and acid treatment can change the structure of SPI, reduce the particle size of protein aggregates and enhance emulsification. Wang et al. [27] used chitosan as a modifier and developed edible composite films of rice protein hydrolysates/chitosan through ultrasound. The results showed that ultrasonic treatment was helpful for film formation and was an effective method to improve the performance of edible composite films. However, the effect of ultrasound on the structure and functional properties of microcapsules prepared under a protein-polysaccharide composite system is still unclear.

Herein, the SPI and MD complex was used to prepare the dispersion system, which was used to embed hemp seed oil and form the emulsion. Then, the emulsion was microencapsulated by spray drying. By studying the microstructure of the composite emulsion under different ultrasonic powers, the morphology and stability of the composite emulsion were investigated, and then the spray-dried microcapsules were analyzed by scanning electron microscopy (SEM), particle size, and Fourier transform infrared (FTIR) spectroscopy to explore the encapsulation effect and functional properties of ultrasound on the microcapsules. The oxidative stability of the embedded hemp seed oil was investigated through oxidation kinetics models, and the mechanism of ultrasound on the formation of microcapsules was analyzed to improve the encapsulation effect and the stability of the microcapsules, which provided conditions for the storage and the stability and slow release of THC.

2. Materials and methods

2.1. Materials

SPI was obtained from Harbin High-Tech Co., Ltd. (Harbin, China). MD (food grade) was purchased from Xiwang Food Co., Ltd. (Shandong, China). Hemp seeds were provided by Shanxi Qinchang Seed Co., Ltd. (Shanxi, China). All other chemicals were commercially available and of analytical grade. An ultrasonic processor (FS-1200 N) was purchased from Shengxi Ultrasonic Instrument Co., Ltd. (Shanghai, China). A spray dryer was obtained from Heilongjiang Heyi Dairy Technology Co., Ltd. (Heilongjiang, China). A fluorescence microscope (Nikon Eclipse TS100) was obtained from Nikon Instruments Inc. (USA). A homogenizer (Ultra-Turrax IKA T18 Basic) was obtained from IKA Works GmbH & Co. (Germany).

2.2. Extraction of HSO

The HSO was extracted according to the method of Shi et al. [28] and was used for subsequent tests.

2.3. Preparation of emulsion

SPI and MD were dispersed in 0.1 M phosphate buffered solution (PBS) with a pH of 7.0 at a mass ratio of 1:1 to form a 10% SPI-MD dispersion. Then, the dispersion was stirred at 200 rpm for 2 h and overnight at 4 °C to ensure that the dispersion could be completely dissolved. Then, the dispersion was incubated at 70 °C for 30 min and cooled to room temperature in an ice bath. HSO (2.5%) was added to the dispersion and homogenized at 14000 rpm for 5 min. The homogenized emulsion was ultrasonically treated in an ice bath (20 kHz, 30 min), and the effect of different ultrasonic powers (0, 150, 300, 450, 600 W) on the characteristics of the emulsion during preparation was studied.

2.4. Characterization of emulsion

2.4.1. Optical microscopy observation

The samples were placed in the center of a clean glass slide and then covered gently with cover glass, and the microstructure of the samples was observed through an optical microscope.

2.4.2. Fluorescence microscopy observation

HSO was fluorescently labeled with Nile red with an excitation wavelength of 543 nm. Then, the type of emulsion was observed with a fluorescence microscope.

2.5. Preparation of microcapsules

The emulsion prepared in the previous step was sent to the spray dryer. The air inlet temperature was 180 °C, the air outlet temperature was 55 °C, the compressed air flow rate was 8 L/min, the diameter of the fluid nozzle was 1.2 mm, and the peristaltic pump flow rate was 0.3 L/h. The prepared microcapsule powder was collected, packaged and stored in an opaque container and placed in a desiccator at 4 °C for further experiments.

2.6. Characterization of microcapsules

2.6.1. SEM observation of microcapsules

The prepared microcapsule powder was placed on a stage with conductive adhesive after drying and then gold-plated (90 s) in a vacuum environment. The microstructure of the microcapsules was observed through SEM.

2.6.2. Determination of particle size of microcapsules

The particle size of the microcapsules was determined according to the method of Timilsena et al. [29]. The prepared microcapsule powder was placed in a container and dispersed in anhydrous ethanol solution with ultrasonication for approximately 5 min. After the sample was uniformly dispersed, the suspended particles were introduced into a Zetasizer-3000HS laser diffractometer for particle size analysis.

2.6.3. FITR analysis

The prepared microcapsules were measured by an 8400S Fourier transform infrared spectrometer. The scanning range was 500–4000 cm^{-1}, 16 scans were performed at room temperature, and the resolution was 8 cm^{-1}.

2.7. Oxidation kinetics models of HSO microcapsules

Numerous studies have shown that the zero-order kinetic model and the first-order kinetic model can describe the quality changes of lipids in food during storage [30]. Therefore, the oxidative stability of HSO microcapsules was studied at the stage when the oil was not obviously leaked, and kinetics models were used to numerically fit the oxidation stability of HSO and HSO microcapsules.

$$\text{Zero} - \text{order kinetic model equation } c = kt + c_0 \quad (1)$$

$$\text{First} - \text{order kinetic model equation } c = c_0 * e^{-kt} \quad (2)$$

where c_0 represents the initial value of peroxide value (POV, mmol/kg), c represents the POV value at t (mmol/kg), k represents the reaction rate constant, and t represents time (d).

2.8. Characteristic analysis of the microcapsules

2.8.1. Determination of powder yield (PY) and encapsulation efficiency (EE)

The PY and EE of the microcapsules were determined according to the methods of Kaushik [31] and Timilsena [29]. Three grams of microcapsule powder was dispersed in 30 mL of n-hexane and vortexed for 60 s, and the surface oil content was measured. Then, the samples were centrifuged at 5000 g for 10 min at ambient temperature. The supernatant was collected, and the solvent (n-hexane) was evaporated and recovered for 12 h. The oil obtained was further heated at 80 °C for 1 h to remove any residual hexane. Then, the oil was cooled to ambient temperature, and the oil content was measured. Three grams of microcapsules was dispersed in 90 mL of 4 mol/L hydrochloric acid, placed in a sealed container, and vortexed for 60 s to determine the total oil content in the microcapsules. Subsequently, n-hexane (45 mL) was added to the mixture and vortexed for an additional 60 s. The mixture was shaken with an orbital shaker for 12 h at room temperature to extract the oil in the solvent phase. Then, the mixture was centrifuged at 10,000 g for 30 min to recover the solvent phase containing dissolved oil. The solvent was distilled, and the remaining oil was dried in an oven at 80 °C to remove the remaining solvent. Finally, the total oil content was determined by the gravimetric method. The PY and EE were calculated as follows:

$$\mathrm{PY}\ (\%) = [\mathrm{HSO}]_{\mathrm{ms}}/[\mathrm{HSO}]_{\mathrm{s}} \times 100\% \tag{3}$$

$$EE\ (\%) = \frac{[HSO]_{total} - [HSO]_{free}}{[HSO]_{total}} \times 100\% \tag{4}$$

where $[\mathrm{HSO}]_{\mathrm{ms}}$ represents the total mass of microcapsule powder collected after spray drying (mg), $[\mathrm{HSO}]_{\mathrm{s}}$ represents the initial mass of solids in the dispersion before spray drying (mg), $[\mathrm{HSO}]_{\mathrm{total}}$ represents the total mass of HSO added into microcapsules (mg), and $[\mathrm{HSO}]_{\mathrm{free}}$ represents the mass of free oil on the surface of microcapsules (mg).

2.8.2. Determination of the degree of glycosylation (DG)

DG was determined based on the O-phthaldialdehyde (OPA) method [32]. OPA (80 mg) was dissolved in 2 mL 95% ethanol and mixed with 50 mL 10 mM sodium tetraborate buffer (pH 9.7), 5 mL 20% sodium dodecyl sulfate (SDS) and 200 μL β-mercaptoethanol. The solution was mixed and diluted with distilled water to a final volume of 100 mL to form OPA reagent. The prepared microcapsules were redissolved in distilled water (2 mg/mL), and then 200 μL was taken and incubated with 4 mL OPA reagent at room temperature for 5 min. The absorbance at 340 nm was determined with an ultraviolet–visible spectrophotometer to obtain the free amino group. Among the samples, the blank was 200 μL distilled water, and 4 mL OPA reagent was added. The DG of the samples was calculated as follows:

$$DG\ (\%) = \frac{A_b - A_s}{A_b} \times 100\% \tag{5}$$

where A_b represents the absorbance of the blank and A_s represents the absorbance of the sample.

2.8.3. Determination of POV

The HSO microcapsules were placed in a thermostat at 20 °C, and the POV was regularly measured. The POV was determined according to the American Oil Chemists' Society (AOCS) official method Cd 8–53 [33].

2.9. Statistical analysis

All the measurements were performed at least in triplicate, and the mean value and standard error were used to analyze the test results. Origin 8.5 was used to record and analyze the data. SPSS 17.0 was used for ANOVA, and Duncan's test ($p < 0.05$) was conducted to evaluate the significance of data differences.

3. Results and discussion

3.1. Effect of ultrasonic power on the characteristics of composite emulsions

3.1.1. Optical microscopy observation of emulsions under different ultrasonic powers

The microstructure of the composite emulsion is one of the key factors affecting the embedding effect of the microcapsules. Optical microscopy can directly reflect the size, dispersion and instability of emulsion droplets. Fig. 1 shows that the SPI-MD and HSO composite emulsion droplets were spherical, and the emulsion droplets without ultrasonic treatment had a large particle size and were not uniform. In comparison, the particle size of the composite emulsion droplets obtained by ultrasound was smaller and more uniform. With increasing ultrasonic power, the particle size of the composite emulsion gradually decreased. When the ultrasonic power was 450 W, the particle size of the emulsion was the smallest because the combination of SPI and MD can form a stable layer of macromolecules around the oil droplets and stabilize the oil droplets through spatial repulsion to prevent flocculation and coalescence [34]. Ultrasound treatment has the functions of mechanical mass transfer, heating and cavitation, which can increase the intermolecular movement between the amino groups of protein and the carboxyl groups of polysaccharide and provide more opportunities for glycosylation of proteins and polysaccharides [35], thereby improving the emulsification of the SPI-MD complex. However, too high ultrasonic power could expose the hydrophobic protein, which caused the aggregation of protein [36], and the emulsification of the complex was decreased.

3.1.2. Fluorescence microscopy observation of emulsions under different ultrasonic powers

From the results of the fluorescence microscopy (Fig. 2), the emulsion of HSO was seen to be labeled with Nile red, the spherical emulsion droplets showed red fluorescence, and the water phase was black, which indicated that HSO had been successfully embedded in the SPI-MD complex, presenting an O/W emulsion. The distribution of emulsion droplets without ultrasonic treatment was found to be more aggregated and varied in size, indicating that the stability was low. With increasing ultrasonic power from 150 to 450 W, the emulsion droplets were gradually dispersed, and the particle size was more uniform because the ultrasonic treatment reduced the aggregation of protein molecules, and the cavitation and turbulence caused by ultrasonic waves effectively broke up the emulsion droplets, resulting in a reduction in particle size. When the ultrasound was excessive, the protein molecules were degraded [37], the continuous protein phase was destroyed, and the MD molecules were also destroyed, forming insoluble aggregates and reducing the amount of emulsifier adsorbed on the surface of the oil droplets, which caused the droplet size to increase and reduced the stability of the emulsion. This result is consistent with the optical microscopy results.

3.2. Effect of ultrasonic power on the characteristics of microcapsules

3.2.1. SEM observation of microcapsules under different ultrasonic powers

The SPI-MD and HSO composite emulsion was spray-dried to prepare microcapsules, and the SEM results are shown in Fig. 3. The microcapsules prepared by the composite emulsion without ultrasonic treatment presented a spherical structure as a whole [38], but the surface of the microcapsules showed some dents and surface damage, and the agglomeration between the microcapsules was obvious. With increasing ultrasonic power, the agglomeration phenomenon between the microcapsules gradually decreased, and the damage to the surface was also reduced because after ultrasonic treatment, the stability of the

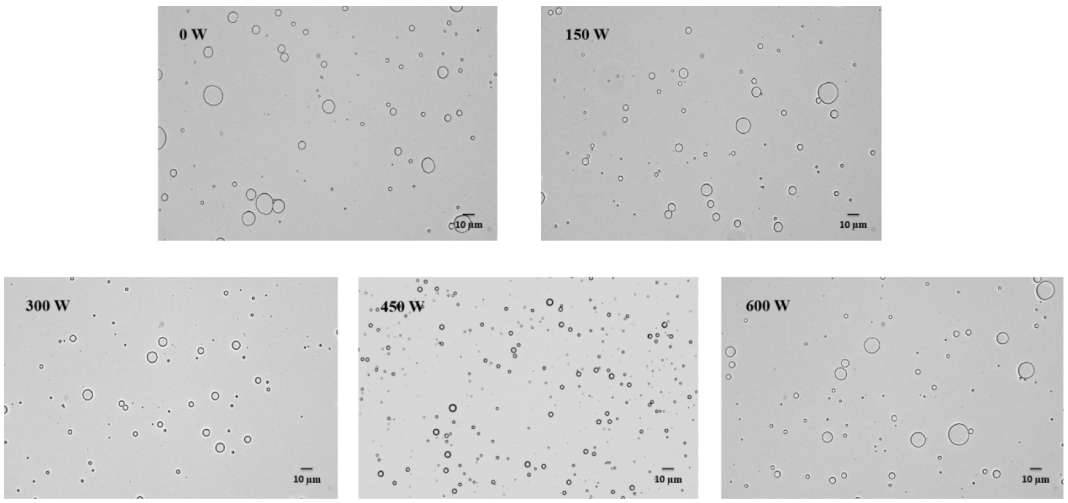

Fig. 1. Optical microscope of composite emulsion under different ultrasonic powers.

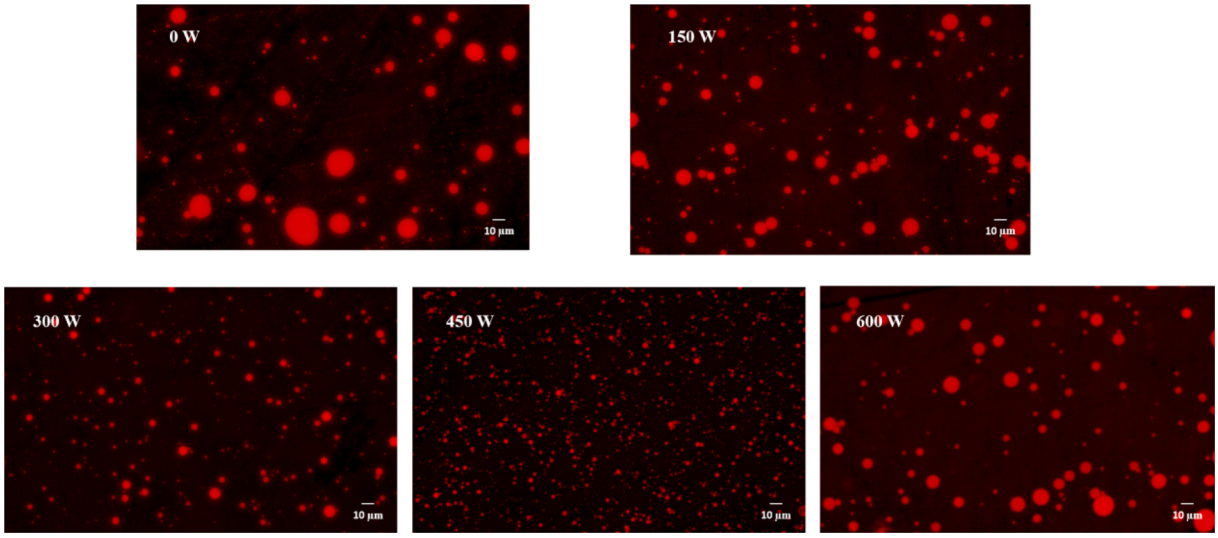

Fig. 2. Fluorescence microscope of composite emulsion under different ultrasonic powers.

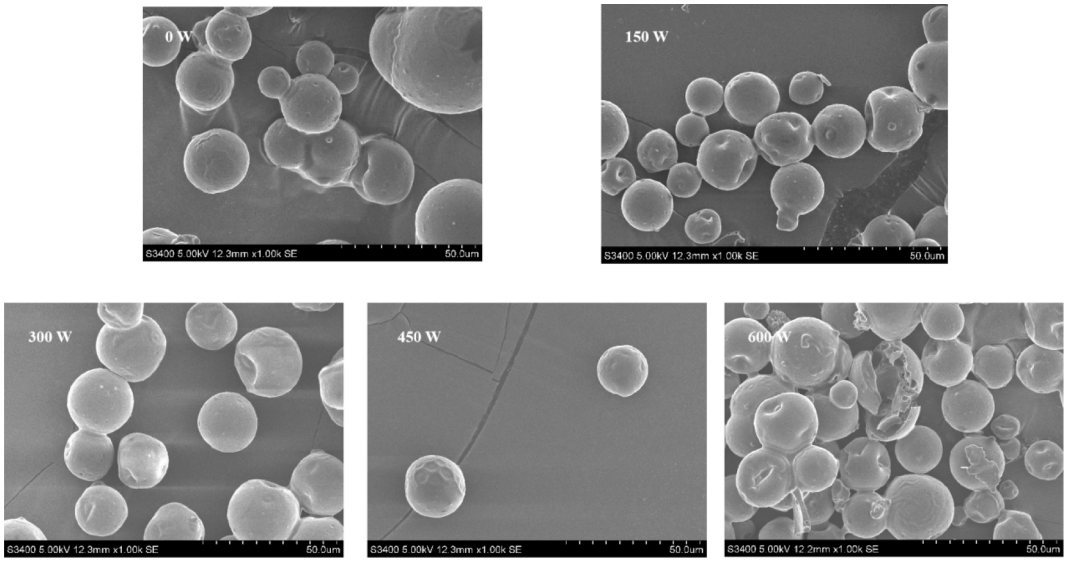

Fig. 3. SEM of microcapsules under different ultrasonic powers

composite emulsion was improved, the coalescence between the emulsion droplets was effectively inhibited, and after spray drying, the microcapsules presented a rounded spherical structure. However, when the ultrasonic power continued to increase, the surface of the microcapsules was obviously damaged, which further indicated that a larger ultrasonic power could destroy the structure of the SPI-MD complex, thereby affecting the structural stability of the microcapsules. This result is consistent with the observation results of optical and fluorescence microscopy and demonstrates that the ultrasonic treatment not only affects the characteristics of the composite emulsion but also has important significance for the formation of microcapsules.

3.2.2. Particle size analysis of microcapsules

The particle size of the microcapsules is shown in Fig. 4. The results showed that the microcapsules had a large particle size and belonged to the micron level [39]. The particle size of the sample without ultrasonic treatment was bimodally distributed, indicating that the particle size distribution was not uniform. With increasing ultrasonic power, the particle size decreased from 20.5 μm to 10.7 μm, caused by shock waves generated by collisions between particles in the emulsion and collapse of cavitation bubbles. From 150 to 450 W, the particle size distribution was narrow and curved, demonstrating that the particle size of the microcapsules obtained by spray drying the composite emulsion after ultrasonic treatment was relatively uniform because the enhancement of ultrasonic power strengthened the collision between the ε-amino groups of the protein and the reducing end of the carbonyl groups of the MD, thereby accelerating the glycosylation reaction, improving the stability of the microcapsule wall materials, preventing the agglomeration of emulsion droplets in the spray drying process, and improving the particle size distribution of the microcapsules. When the ultrasonic power was 600 W, the particle size distribution of the microcapsules was wider, which may be due to the aggregation of composite emulsion droplets during the spray drying process. High-power ultrasonic treatment caused protein folding, which led to the re-embedding of free amino acid groups and reduced the degree of glycosylation, thereby causing the aggregation of emulsion droplets. This phenomenon can be called the "overtreatment effect" [40], which slightly increased the particle size of the microcapsules. The result is consistent with the results of SEM.

3.2.3. FTIR analysis of microcapsules

The FTIR analysis of HSO microcapsules is shown in Fig. 5. The microcapsule samples all showed absorption peaks at 1658 (amide I), 1542 (amide II) and 1405 cm^{-1} (amide III), corresponding to C-O stretching vibration, N–H bending vibration and C-N stretching vibration, respectively. These results are consistent with the report on SPI by Huang et al. [41]. Moreover, the absorption intensity of the amide I, II, and III bands was relatively large, indicating that the covalent bonding of SPI and MD through the Maillard reaction affected the vibration of the amide groups. In addition, compared with nonultrasonic samples, ultrasonic treatment changed the structure of the internal groups of the microcapsule wall materials but did not damage its original basic structure. With increasing ultrasonic power, the peak intensities at 1021 cm^{-1} and 1161 cm^{-1} increased, which was related to the stretching vibration of the C-O-C glycosidic bond [42]. Ultrasonic treatment may also increase the absorption peak intensity at 2931 cm^{-1} and 3406 cm^{-1} to a certain extent, which was caused by the introduction of CH_3 and CH_2 groups in the polysaccharide chain that promote the C–H stretching vibration [43]. The results prove that ultrasonic treatment can strengthen the interaction between SPI and MD, thereby showing a certain influence on the molecular structure of HSO microcapsules formed by the SPI-MD complex.

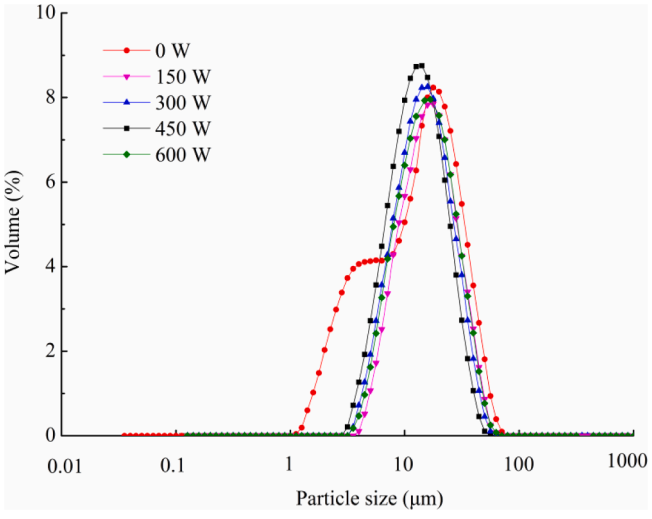

Fig. 4. Particle size distribution of microcapsules under different ultrasonic powers.

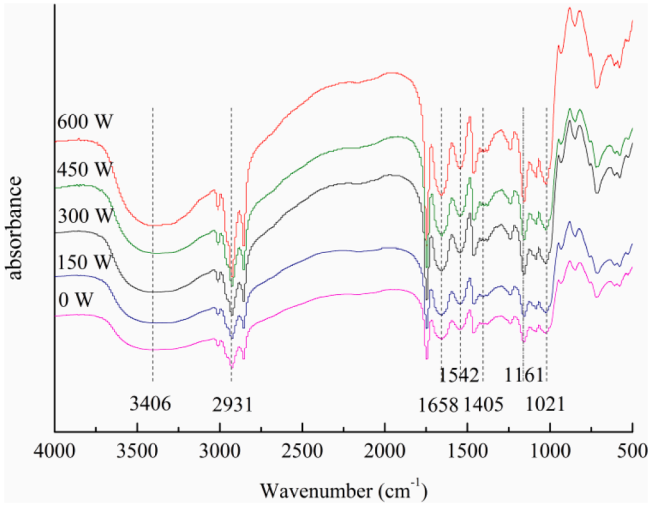

Fig. 5. FTIR analysis of microcapsules under different ultrasonic powers.

3.2.4. Determination of DG of SPI-MD, PY and EE of microcapsules under different ultrasonic powers

According to the methods in 2.3 and 2.5, HSO microcapsules were prepared under optimal conditions, and the encapsulation effects are shown in Table 1. The data showed that DG was in the range of 4.77–15.82%; with increasing ultrasonic power, DG first increased and then decreased, and the DG of the complex after ultrasonic treatment was significantly higher than the DG of the complex without ultrasonic treatment. The results are consistent with the findings reported by Li et al. [44]. The PY of the microcapsules after spray drying was 45.43–67.54%, consistent with the report of Kaushik et al. [31]. In the spray drying process, solid loss is inevitable, mainly including the powder in the cyclone separator, the powder adhering to the wall of the

Table 1
DG (degree of glycosylation) of SPI-MD (soy protein isolate-maltodextrin), PY (powder yield) and EE (encapsulation efficiency) of microcapsules under different ultrasonic powers.

Ultrasonic powers(W)	DG (%)	PY (%)	EE (%)
0	4.77 ± 0.75^{d}	45.43 ± 0.96^{e}	77.32 ± 0.94^{d}
150	9.72 ± 0.58^{c}	51.55 ± 1.22^{c}	87.66 ± 1.02^{c}
300	12.35 ± 0.83^{b}	59.87 ± 1.74^{b}	92.02 ± 1.35^{b}
450	15.82 ± 0.96^{a}	67.54 ± 2.10^{a}	95.32 ± 1.62^{a}
600	5.66 ± 0.61^{d}	49.88 ± 0.89^{d}	83.72 ± 1.22^{e}

Note: The values with different superscript letters within a column are significantly different ($p < 0.05$).

drying chamber and the sediment at the bottom of the drying chamber [45], so that the solid loss determines the yield of the powder. EE presents the percentage of encapsulated oil in microcapsules, which refers to the percentage of encapsulated oil in the total oil (including surface oil and encapsulated oil). In general, the HSO microcapsules formed by the SPI-MD complex had a higher EE (95.32%) when the ultrasonic power was 450 W.

3.3. Mechanism of ultrasound on the emulsion and wall materials of microcapsules

The covalent bond between SPI and MD was based on the Maillard reaction between the free amino groups of the protein and the reducing end carbonyl groups of MD. After embedding HSO with SPI-MD as the wall material, an O/W composite emulsion was formed. Ultrasonic treatment acted on the composite emulsion to improve the emulsification effect of the emulsion and reduce the particle size of the emulsion droplets (Fig. S1). The thermal, mechanical and chemical effects of ultrasonic treatment are attributed to the rapid formation and collapse of cavitation bubbles in the liquid at high water activity. These bubbles collapse in the positive pressure cycle, creating highly turbulent flow conditions and extremely high pressure and temperature, leading to a stretch of the protein structure and providing more free amino groups to covalently bind to MD. Ultrasonic treatment also has an important impact on the stability and embedding effect of the spray-dried microcapsules. The study found that compared with the microcapsules without ultrasonic treatment, after ultrasonic treatment, the combination of SPI and MD was tighter, and the DG of the complex was significantly improved. Fig. 6 shows that SPI formed a loose adsorption on the interface, and each molecule occupied a large area. After glycosylation with MD, the number of adsorption sites decreased, and the area occupied by each molecule was smaller than the area occupied by each molecule of SPI; however, the adsorption capacity increased. Ultrasonic treatment dispersed the aggregates, the complex occupied a small area on the interface, and its steric hindrance was small, which promoted the intermolecular movement between the amino groups of SPI and the carboxyl group of MD [46] and made the complex tend to pack tightly, forming a thicker interfacial film.

3.4. Oxidation kinetics models of HSO microcapsules

Lipid oxidation kinetics models can well predict the degree of lipid oxidation deterioration [47]. The experiment found that a certain amount of oil leaked on the surface of the HSO microcapsules after storage at a constant temperature of 20 °C for 30 d, but no rancidity or peculiar smell appeared. Therefore, the study was carried out on HSO and HSO microcapsules stored for 30 d. POV oxidation kinetics models in this period were constructed. The study used the zero-order model and the first-order model to fit the POV of HSO and HSO microcapsules. The results are shown in Table 2.

As shown in Table 2, under the same conditions, the correlation coefficients of the first-order model fitting equation of HSO were higher than the correlation coefficients of the zero-order model fitting equation, and the first-order model had a higher degree of fit. The correlation coefficients of the zero-order model fitting equation of HSO microcapsules were all higher than the correlation coefficients of the first-order model fitting equation, and the fitting degree of the zero-order model was higher. In addition, the regression equations were linearly correlated, and the correlation degree was significant, indicating that the HSO microcapsules had better oxidation stability.

To verify the feasibility of the kinetics models, a set of parallel test data with storage times of 5, 10, and 30 d was randomly selected and compared with the predicted values obtained from the optimized model, and the relative error range values were calculated. The results are shown in Table 3. Unencapsulated HSO had a large prediction error of POV on the 30th day (6.44%), while the optimization model of HSO microcapsules had a small relative error between the predicted value and the experimental value. The established model can better reflect the quality changes and predict the degree of lipid oxidation during the storage of HSO microcapsules.

4. Conclusions

Microcapsule-embedded HSO with SPI and MD was successfully prepared by spray drying. The effect of ultrasonic treatment on the microstructure and characteristics of composite emulsions and microcapsules during the preparation process was investigated. Ultrasonic treatment was found to be able to increase the covalent bonding degree of SPI and MD, significantly reduce the particle size of the emulsion, and improve the emulsification and stability of the emulsion. The DG of SPI-MD, PY and EE of microcapsules treated with 450 W ultrasound were all at a relatively high level. Through the construction and verification of the oxidation kinetics models, the HSO microcapsules were determined to have good oxidation stability. The kinetic model could be used to predict the change in POV during the storage of HSO microcapsules, and the model had a good degree of fit, which provided the possibility to predict and regulate the degree of lipid oxidation of HSO microcapsules during storage and provided a basis for the sustained release of THC microcapsules in the future.

Declaration of Competing Interest

The authors declare that they have no known competing financial interests or personal relationships that could have appeared to influence

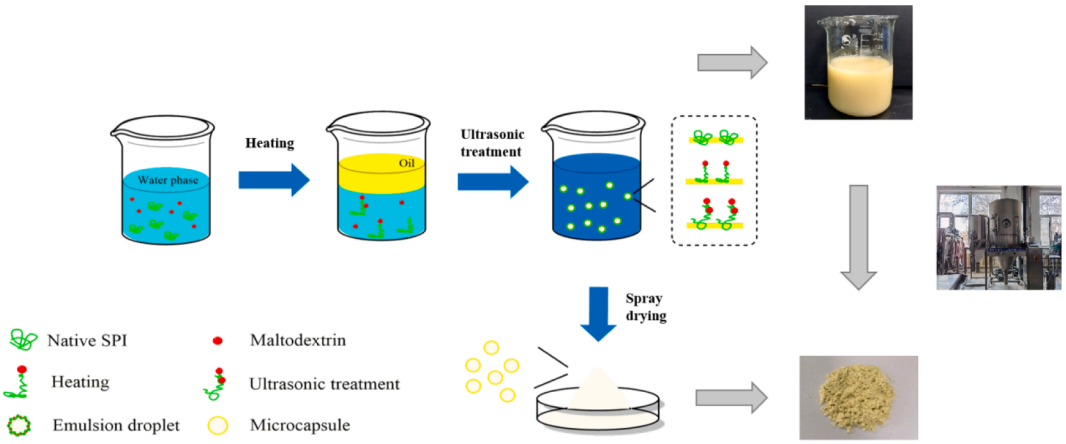

Fig. 6. Mechanism of the effect of ultrasonic treatment on the adsorption layer of the oil–water interface bond.

Table 2
Regression equations of POV (peroxide value) of HSO (hemp seed oil) and HSO microcapsules.

sample	Zero-order		First-order	
	Fitting equation	R^2_{adj}	Fitting equation	R^2_{adj}
HSO	c = 0.29705*t + 1.18762	0.94938	c = 2.1233*exp (0.05506*t)	0.9973
HSO microcapsules	c = 0.1371*t + 2.07524	0.99533	c = 2.40574*exp (0.03254*t)	0.97006

Table 3
Validation of oxidation kinetics models.

sample	HSO	HSO microcapsules
Optimal model	c = 2.1233*exp (0.05506*t)	c = 0.1371*t + 2.07524
Storage for 5 d (predicted)	2.80	2.76
Storage for 5 d (experimental)	2.93	2.69
Storage for 10 d (predicted)	3.68	3.45
Storage for 10 d (experimental)	3.62	3.56
Storage for 30 d (predicted)	10.41	6.18
Storage for 30 d (experimental)	11.08	6.23
Range of 3 experiments of relative error/%	1.63–6.44	0.81–3.19

the work reported in this paper.

Acknowledgements

This work was supported by a grant from the National Natural Science Foundation of China (NSFC): Construction of a three-dimensional enzyme electrode and its correlation with phospholipid content in oil (No: **32072259**).

Appendix A. Supplementary data

Supplementary data to this article can be found online at https://doi.org/10.1016/j.ultsonch.2021.105700.

References

[1] A. Pratap Singh, F. Fathordoobady, Y. Guo, A. Singh, D.D. Kitts, Antioxidants help favorably regulate the kinetics of lipid peroxidation, polyunsaturated fatty acids degradation and acidic cannabinoids decarboxylation in hempseed oil, Sci. Rep. 10 (2020) 10567, https://doi.org/10.1038/s41598-020-67267-0.
[2] B. Matthäus, L. Brühl, Virgin hemp seed oil: An interesting niche product, Eur. J. Lipid Sci. Technol. 110 (7) (2008) 655–661, https://doi.org/10.1002/ejlt.v110:710.1002/ejlt.200700311.
[3] G. Crescente, S. Piccolella, A. Esposito, M. Scognamiglio, A. Fiorentino, S. Pacifico, Chemical composition and nutraceutical properties of hempseed: an ancient food with actual functional value, Phytochem. Rev. 17 (4) (2018) 733–749, https://doi.org/10.1007/s11101-018-9556-2.
[4] Q. Luo, X. Yan, L. Bobrovskaya, M. Ji, H. Yuan, H. Lou, P. Fan, Anti-neuroinflammatory effects of grossamide from hemp seed via suppression of TLR-4-mediated NF-κB signaling pathways in lipopolysaccharide-stimulated BV2 microglia cells, Mol. Cell. Biochem. 428 (1-2) (2017) 129–137, https://doi.org/10.1007/s11010-016-2923-7.
[5] A. Smeriglio, E.M. Galati, M.T. Monforte, F. Lanuzza, V. D'Angelo, C. Circosta, Polyphenolic compounds and antioxidant activity of cold-pressed seed oil from finola cultivar of *Cannabis sativa* L, Phytother. Res. 30 (8) (2016) 1298–1307, https://doi.org/10.1002/ptr.v30.810.1002/ptr.5623.
[6] X. Yan, J. Tang, C. dos Santos Passos, A. Nurisso, C.A. Simões-Pires, M. Ji, H. Lou, P. Fan, Characterization of Lignanamides from Hemp (Cannabis sativa L.) seed and their antioxidant and acetylcholinesterase inhibitory activities, J. Agric. Food Chem. 63 (49) (2015) 10611–10619, https://doi.org/10.1021/acs.jafc.5b05282.
[7] T. Chen, J. He, J. Zhang, H. Zhang, P. Qian, J. Hao, L. Li, Analytical characterization of hempseed (Seed of *Cannabis sativa* L.) oil from eight regions in China, J. Diet. Suppl. 7 (2) (2010) 117–129, https://doi.org/10.3109/19390211003781669.
[8] C. Chuang, A. Ye, S.G. Anema, S.M. Loveday, Concentrated Pickering emulsions stabilised by hemp globulin-caseinate nanoparticles: tuning the rheological properties by adjusting the hemp globulin: caseinate ratio, Food Funct. 11 (2020) 10193–10204, https://doi.org/10.1039/D0FO01745K.
[9] A.T. Girgih, C.C. Udenigwe, R.E. Aluko, In vitro antioxidant properties of hemp seed (*Cannabis sativa* L.) protein hydrolysate fractions, J. Am. Oil Chem. Soc. 88 (3) (2011) 381–389, https://doi.org/10.1007/s11746-010-1686-7.
[10] N. De Briyne, D. Holmes, I. Sandler, E. Stiles, D. Szymanski, S. Moody, S. Neumann, A. Anadon, Cannabis, cannabidiol oils and tetrahydrocannabinol-what do veterinarians need to know? Animals 11 (3) (2021) 892, https://doi.org/10.3390/ani11030892.
[11] S.G. Meuth, T. Henze, U. Essner, C. Trompke, C. Vila Silván, Tetrahydrocannabinol and cannabidiol oromucosal spray in resistant multiple sclerosis spasticity: consistency of response across subgroups from the SAVANT randomized clinical trial, Int. J. Neurosci. 130 (12) (2020) 1199–1205, https://doi.org/10.1080/00207454.2020.1730832.
[12] A. Escudero-Lara, J. Argerich, D. Cabañero, R. Maldonado, Disease-modifying effects of natural Δ9-tetrahydrocannabinol in endometriosis-associated pain, eLife 9 (2020) e50356, https://doi.org/10.1101/715938.
[13] L. Izzo, S. Pacifico, S. Piccolella, L. Castaldo, A. Narváez, M. Grosso, A. Ritieni, Chemical analysis of minor bioactive components and cannabidiolic acid in commercial hemp seed oil, Molecules 25 (2020) 3710, https://doi.org/10.3390/molecules25163710.
[14] S.A. Hogan, B.F. McNamee, E.D. O'Riordan, M. O'Sullivan, Emulsification and microencapsulation properties of sodium caseinate/carbohydrate blends, Int. Dairy J. 11 (3) (2001) 137–144, https://doi.org/10.1016/S0958-6946(01)00091-7.
[15] X. Chen, R. Liang, F. Zhong, J. Ma, N.-A. John, H.D. Goff, W.H. Yokoyama, Effect of high concentrated sucrose on the stability of OSA-starch-based beta-carotene microcapsules, Food Hydrocoll. 113 (2021) 105472, https://doi.org/10.1016/j.foodhyd.2019.105472.
[16] A. Elik, D. Koçak Yanık, F. Göğüş, A comparative study of encapsulation of carotenoid enriched-flaxseed oil and flaxseed oil by spray freeze-drying and spray drying techniques, LWT-Food, Sci. Technol. 143 (2021) 111153, https://doi.org/10.1016/j.lwt.2021.111153.
[17] W. Shao, X. Pan, X. Liu, F. Teng, S. Yuan, Microencapsulation of docosahexaenoic acid algal oil using spray drying technology, Food Technol. Biotechnol. 56 (1) (2018), https://doi.org/10.17113/ftb10.17113/ftb.56.01.18.5452.
[18] M.E. Rodríduez Huezo, R. Pedroza Islas, L.A. Prado Barragán, C.I. Beristain, E. J. Vernon Carter, Microencapsulation by spray drying of multiple emulsions containing carotenoids, J. Food Sci. 69 (2004) 351–359, https://doi.org/10.1111/j.1365-2621.2004.tb13641.x.
[19] X. Zhang, Y. Lei, X. Luo, Y. Wang, Y. Li, B. Li, S. Liu, Impact of pH on the interaction between soybean protein isolate and oxidized bacterial cellulose at oil-water interface: Dilatational rheological and emulsifying properties, Food Hydrocoll. 115 (2021) 106609, https://doi.org/10.1016/j.foodhyd.2021.106609.
[20] S.K. Wong, J. Supramaniam, T.W. Wong, A. Soottitantawat, U.R. Ruktanonchai, B. T. Tey, S.Y. Tang, Synthesis of bio-inspired cellulose nanocrystals-soy protein isolate nanoconjugate for stabilization of oil-in-water Pickering emulsions, Carbohydr. Res. 504 (2021) 108336, https://doi.org/10.1016/j.carres.2021.108336.
[21] M.C. Otálora, J.G. Carriazo, L. Iturriaga, M.A. Nazareno, C. Osorio, Microencapsulation of betalains obtained from cactus fruit (Opuntia ficus-indica) by spray drying using cactus cladode mucilage and maltodextrin as encapsulating agents, Food Chem. 187 (2015) 174–181, https://doi.org/10.1016/j.foodchem.2015.04.090.
[22] T.S. Awad, H.A. Moharram, O.E. Shaltout, D. Asker, M.M. Youssef, Applications of ultrasound in analysis, processing and quality control of food: A review, Food Res. Int. 48 (2) (2012) 410–427, https://doi.org/10.1016/j.foodres.2012.05.004.
[23] E.K. Silva, M.A.A. Meireles, Influence of the degree of inulin polymerization on the ultrasound-assisted encapsulation of annatto seed oil, Carbohydr. Polym. 133 (2015) 578–586, https://doi.org/10.1016/j.carbpol.2015.07.025.
[24] X.i. Niu, C. Zhao, Q. Shi, S. Wang, Y. Zhao, S. Li, H. Yin, N. Lin, J. Liu, Effect of ultrasonic treatment on peanut protein isolate-oat dietary fibre mixture gels induced by transglutaminase, Int. J. Food Sci. Technol. 56 (5) (2021) 2233–2243, https://doi.org/10.1111/ijfs.v56.510.1111/ijfs.14839.
[25] J. Gu, Q. Li, J. Liu, Z. Ye, T. Feng, G. Wang, W. Wang, Y. Zhang, Ultrasonic–assisted extraction of polysaccharides from Auricularia auricula and effects of its acid hydrolysate on the biological function of Caenorhabditis elegans, Int. J. Biol. Macromol. 167 (2021) 423–433, https://doi.org/10.1016/j.ijbiomac.2020.11.160.
[26] L. Huang, X. Ding, Y. Li, H. Ma, The aggregation, structures and emulsifying properties of soybean protein isolate induced by ultrasound and acid, Food Chem. 279 (2019) 114–119, https://doi.org/10.1016/j.foodchem.2018.11.147.
[27] L. Wang, J. Ding, Y. Fang, X. Pan, F. Fan, P. Li, Q. Hu, Effect of ultrasonic power on properties of edible composite films based on rice protein hydrolysates and chitosan, Ultrason. Sonochem. 65 (2020) 105049, https://doi.org/10.1016/j.ultsonch.2020.105049.
[28] Y. Shi, W. Wang, X. Zhu, B. Wang, Y. Hao, L. Wang, D. Yu, W. Elfalleh, Preparation and physicochemical stability of hemp seed oil liposomes, Ind. Crops Prod. 162 (2021) 113283, https://doi.org/10.1016/j.indcrop.2021.113283.
[29] Y.P. Timilsena, R. Adhikari, C.J. Barrow, B. Adhikari, Microencapsulation of chia seed oil using chia seed protein isolate chia seed gum complex coacervates, Int. J.

Biol. Macromol. 91 (2016) 347–357, https://doi.org/10.1016/j.ijbiomac.2016.05.058.
[30] J.-W. Bai, Z.-J. Gao, H.-W. Xiao, X.-T. Wang, Q. Zhang, Polyphenol oxidase inactivation and vitamin C degradation kinetics of Fuji apple quarters by high humidity air impingement blanching, Int. J. Food Sci. Technol. 48 (6) (2013) 1135–1141, https://doi.org/10.1111/ijfs.2013.48.issue-610.1111/j.1365-2621.2012.03193.x.
[31] P. Kaushik, K. Dowling, S. McKnight, C.J. Barrow, B. Adhikari, Microencapsulation of flaxseed oil in flaxseed protein and flaxseed gum complex coacervates, Food Res. Int. 86 (2016) 1–8, https://doi.org/10.1016/j.foodres.2016.05.015.
[32] M.S. Vigo, L.S. Malec, R.G. Gomez, R.A. Llosa, Spectrophotometric assay using o-phthaldialdehyde for determination of reactive lysine in dairy products, Food Chem. 44 (5) (1992) 363–365, https://doi.org/10.1016/0308-8146(92)90269-8.
[33] AOCS, Official Method and Recommended Practices of the American Oil Chemists' Society, American Oil Chemists' Society, Champaign, IL, 2009.
[34] S. Pirestani, A. Nasirpour, J. Keramat, S. Desobry, Preparation of chemically modified canola protein isolate with gum Arabic by means of Maillard reaction under wet-heating conditions, Carbohydr. Polym. 155 (2017) 201–207, https://doi.org/10.1016/j.carbpol.2016.08.054.
[35] H. Zhang, J. Yang, Y. Zhao, High intensity ultrasound assisted heating to improve solubility, antioxidant and antibacterial properties of chitosan-fructose Maillard reaction products, LWT-Food Sci. Technol. 60 (1) (2015) 253–262, https://doi.org/10.1016/j.lwt.2014.07.050.
[36] J.A. Resendiz-Vazquez, J.A. Ulloa, J.E. Urías-Silvas, P.U. Bautista-Rosales, J. C. Ramírez-Ramírez, P. Rosas-Ulloa, L. González-Torres, Effect of high-intensity ultrasound on the technofunctional properties and structure of jackfruit (Artocarpus heterophyllus) seed protein isolate, Ultrason. Sonochem. 37 (2017) 436–444, https://doi.org/10.1016/j.ultsonch.2017.01.042.
[37] Y. Xiong, Q. Li, S. Miao, Y. Zhang, B. Zheng, L. Zhang, Effect of ultrasound on physicochemical properties of emulsion stabilized by fish myofibrillar protein and xanthan gum, Innov. Food Sci. Emerg. Technol. 54 (2019) 225–234, https://doi.org/10.1016/j.ifset.2019.04.013.
[38] M. Mehran, S. Masoum, M. Memarzadeh, Microencapsulation of Mentha spicata essential oil by spray drying: Optimization, characterization, release kinetics of essential oil from microcapsules in food models, Ind. Crops Prod. 154 (2020) 112694, https://doi.org/10.1016/j.indcrop.2020.112694.
[39] L.B. Pham, B.o. Wang, B. Zisu, T. Truong, B. Adhikari, Microencapsulation of flaxseed oil using polyphenol-adducted flaxseed protein isolate-flaxseed gum complex coacervates, Food Hydrocoll. 107 (2020) 105944, https://doi.org/10.1016/j.foodhyd.2020.105944.
[40] S. Kentish, T.J. Wooster, M. Ashokkumar, S. Balachandran, R. Mawson, L. Simons, The use of ultrasonics for nanoemulsion preparation, Innov. Food Sci. Emerg. Technol. 9 (2) (2008) 170–175, https://doi.org/10.1016/j.ifset.2007.07.005.
[41] G.-Q. Huang, Y.-T. Sun, J.-X. Xiao, J. Yang, Complex coacervation of soybean protein isolate and chitosan, Food Chem. 135 (2) (2012) 534–539, https://doi.org/10.1016/j.foodchem.2012.04.140.
[42] J. Liu, Q. Ru, Y. Ding, Glycation a promising method for food protein modification: Physicochemical properties and structure, a review, Food Res. Int. 49 (1) (2012) 170–183, https://doi.org/10.1016/j.foodres.2012.07.034.
[43] Q. Liu, B. Kong, J. Han, C. Sun, P. Li, Structure and antioxidant activity of whey protein isolate conjugated with glucose via the Maillard reaction under dry-heating conditions, Food Struct. 1 (2) (2014) 145–154, https://doi.org/10.1016/j.foostr.2013.11.004.
[44] C. Li, H. Xue, Z. Chen, Q. Ding, X. Wang, Comparative studies on the physicochemical properties of peanut protein isolate–polysaccharide conjugates prepared by ultrasonic treatment or classical heating, Food Res. Int. 57 (2014) 1–7, https://doi.org/10.1016/j.foodres.2013.12.038.
[45] L.H. Tan, L.W. Chan, P.W.S. Heng, Effect of oil loading on microspheres produced by spray drying, J. Microencapsul. 22 (3) (2005) 253–259, https://doi.org/10.1080/02652040500100329.
[46] N. Kardos, J.-L. Luche, Sonochemistry of carbohydrate compounds, Carbohydr. Res. 332 (2) (2001) 115–131, https://doi.org/10.1016/S0008-6215(01)00081-7.
[47] S.D. Shim, S.J. Lee, Shelf-life prediction of perilla oil by considering the induction period of lipid oxidation, Eur. J. Lipid Sci. Technol. 113 (7) (2011) 904–909, https://doi.org/10.1002/ejlt.201000325.